Supplementary Information

Gas-Phase Growth of Two-Dimensional Nonlayered Metallic Cu_2Se Nanoflakes for Ultrasensitive Surface-Enhanced Raman Scattering

Guiying Li,[†a] Yuying Wang,[†a] Ning Zhou,[a] Chenying Yang,[a] Yuchuan Shao,[ab] and Tao Liang[*a]

[a] Hangzhou Institute for Advanced Study, University of Chinese Academy of Sciences, Hangzhou 310024, China. E-mail: liangtao@ucas.ac.cn

[b] Key Laboratory of Materials for High-Power Laser, Shanghai Institute of Optics and Fine Mechanics, Chinese Academy of Sciences, Shanghai 201800, China.

[†] These authors contributed equally to this work.

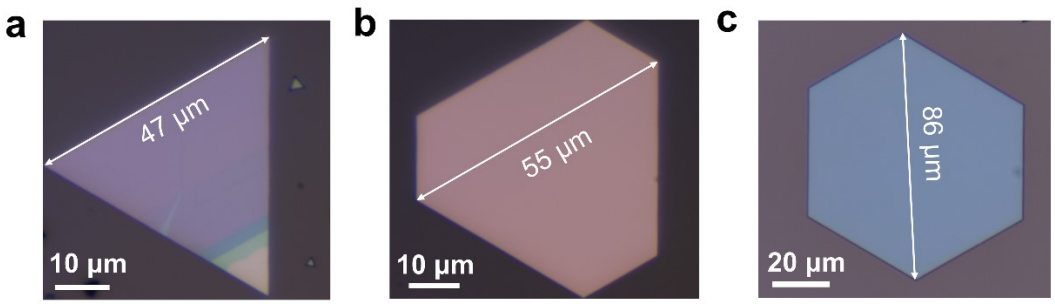

Figure S1. OM images of 2D Cu_2Se nanoflakes with (a) triangular, (b) truncated triangular, and (c) hexagonal morphologies, showing the corresponding lateral sizes.

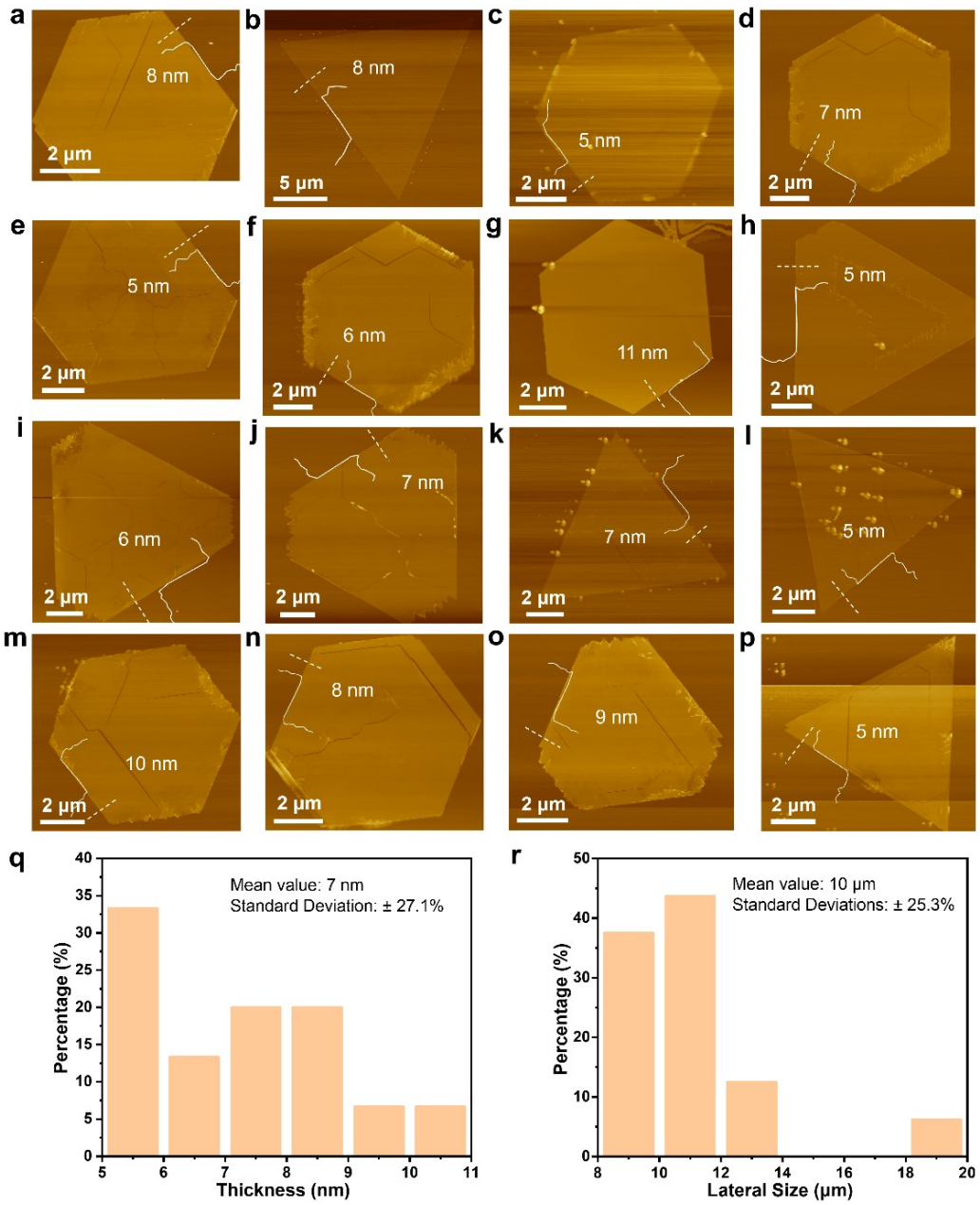

Figure S2. Statistical evaluation of both the lateral size and thickness distributions of the Cu_2Se nanoflakes. (a-p) AFM height images of multiple Cu_2Se nanoflakes synthesized under the optimal growth conditions. (q) Histogram of the thickness distribution. (r) Histogram of the lateral size distribution.

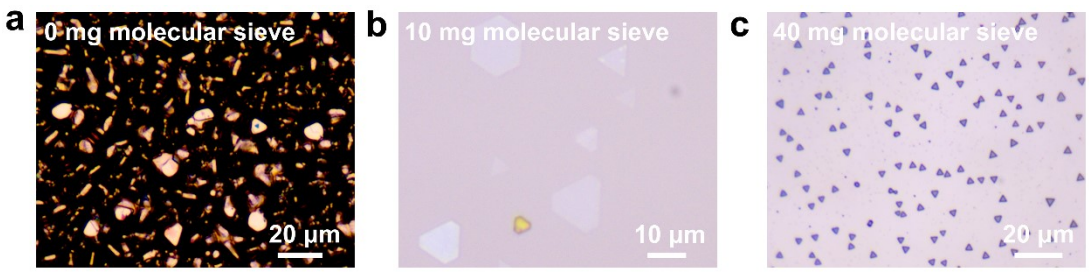

Figure S3. OM images of Cu_2Se nanoflakes synthesized with varied masses of molecular sieve: (a) 0, (b) 10, and (c) 40 mg, respectively.

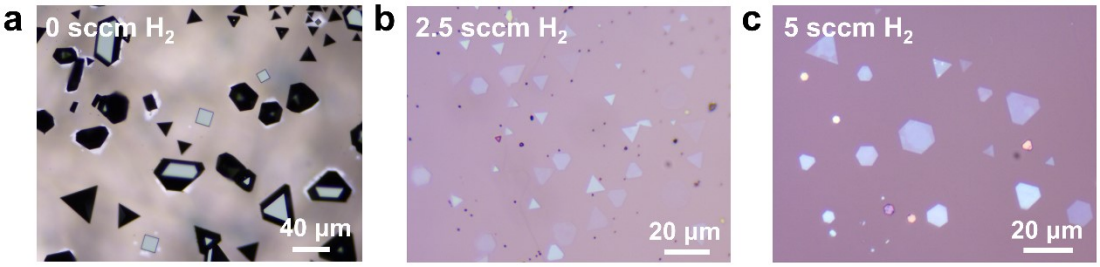

Figure S4. Cu_2Se nanoflakes synthesized with different H_2 concentrations in the carrier gas (Ar/H_2 mixture). (a-c) The H_2 partial flow rates are 0, 2.5, and 5 sccm as labeled, respectively.

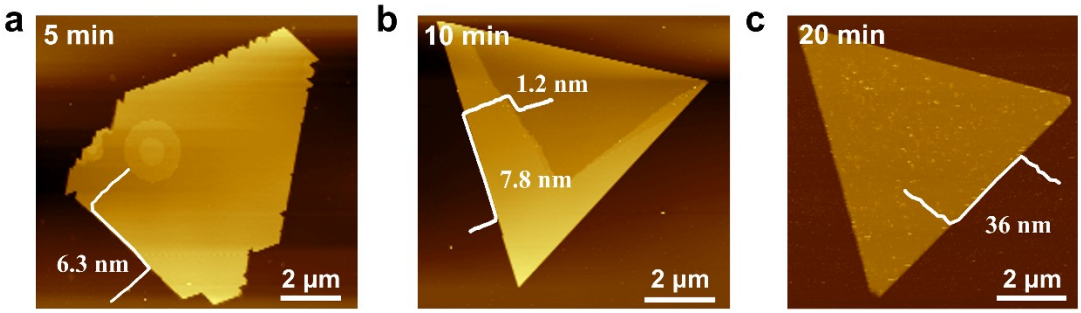

Figure S5. AFM images of Cu_2Se nanoflakes grown for (a) 5 min, (b) 10 min, and (c) 20 min, respectively.

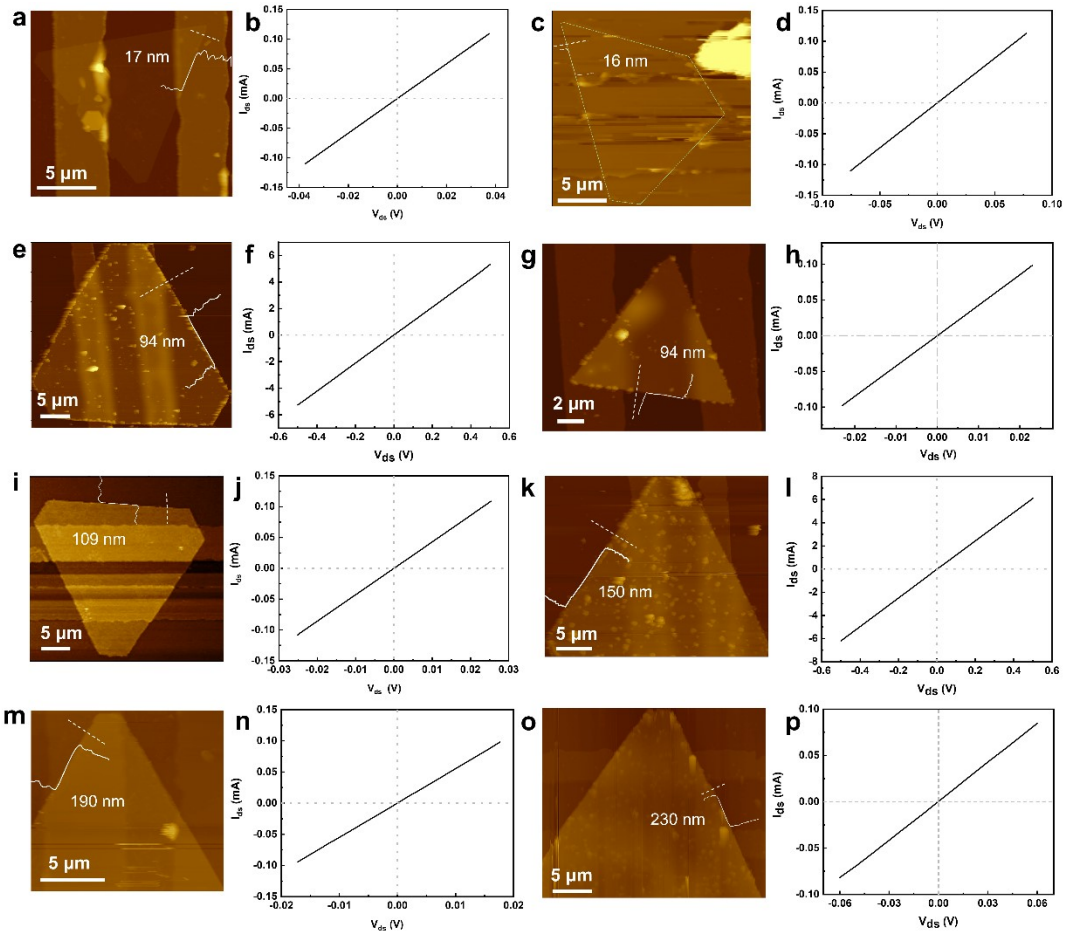

Figure S6. AFM height images and corresponding output characteristics of Cu_2Se FET devices with different thicknesses.

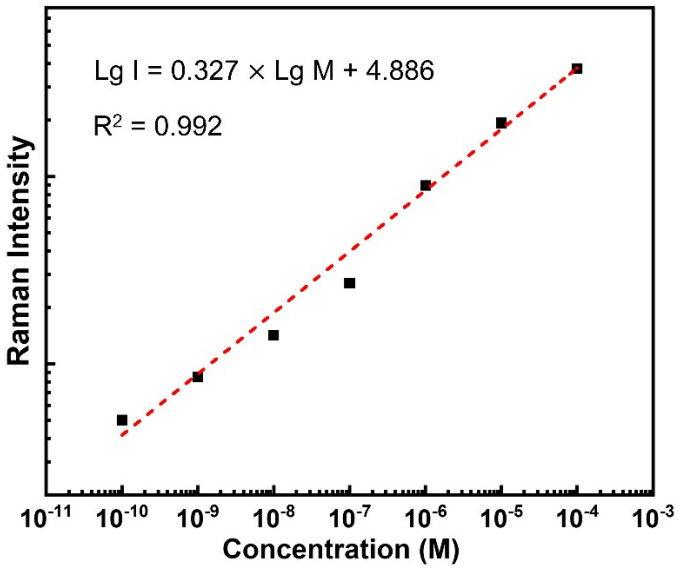

Figure S7. Raman intensity as a function of MB concentration.

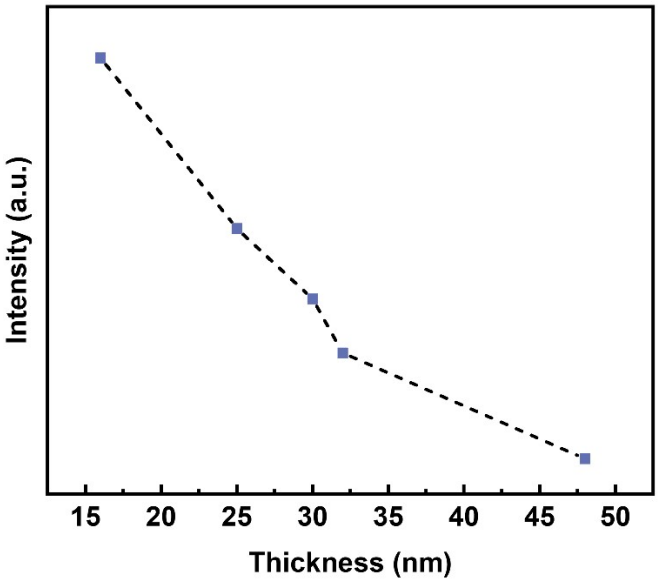

Figure S8. Thickness-dependent SERS Raman intensity of Cu_2Se nanoflakes.

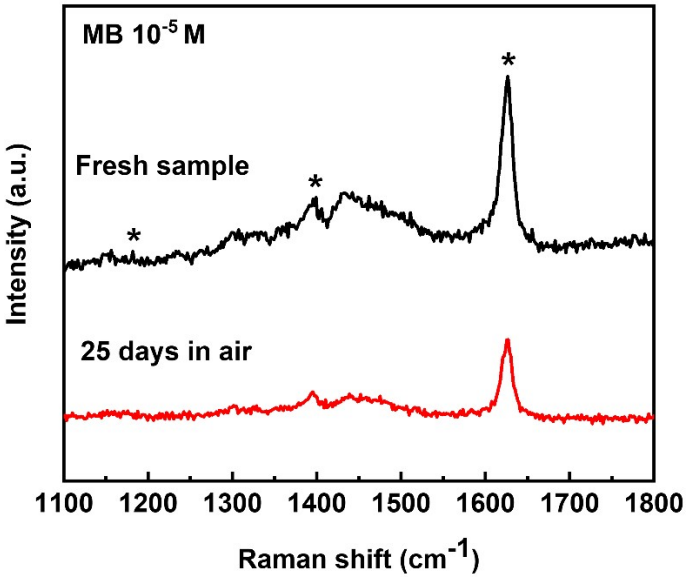

Figure S9. Comparison of Raman spectra of MB (10^{-5} M) on Cu_2Se nanoflake after exposure to ambient air for 25 days.

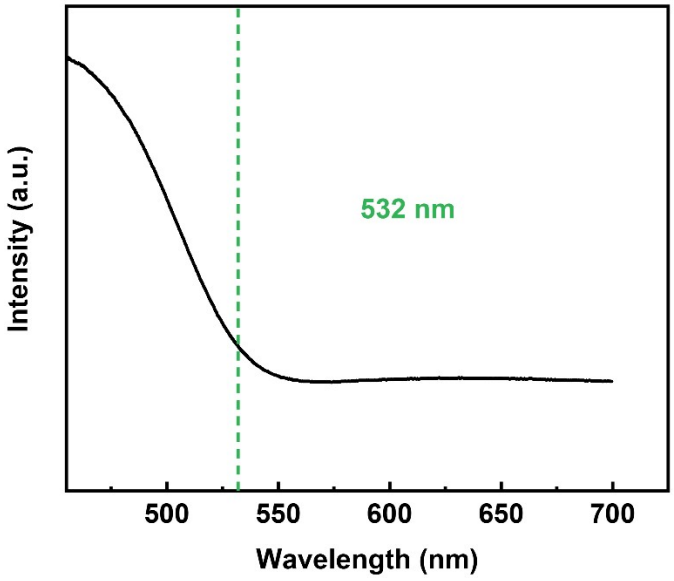

Figure S10. UV-Vis absorption spectrum of Cu_2Se nanoflakes.

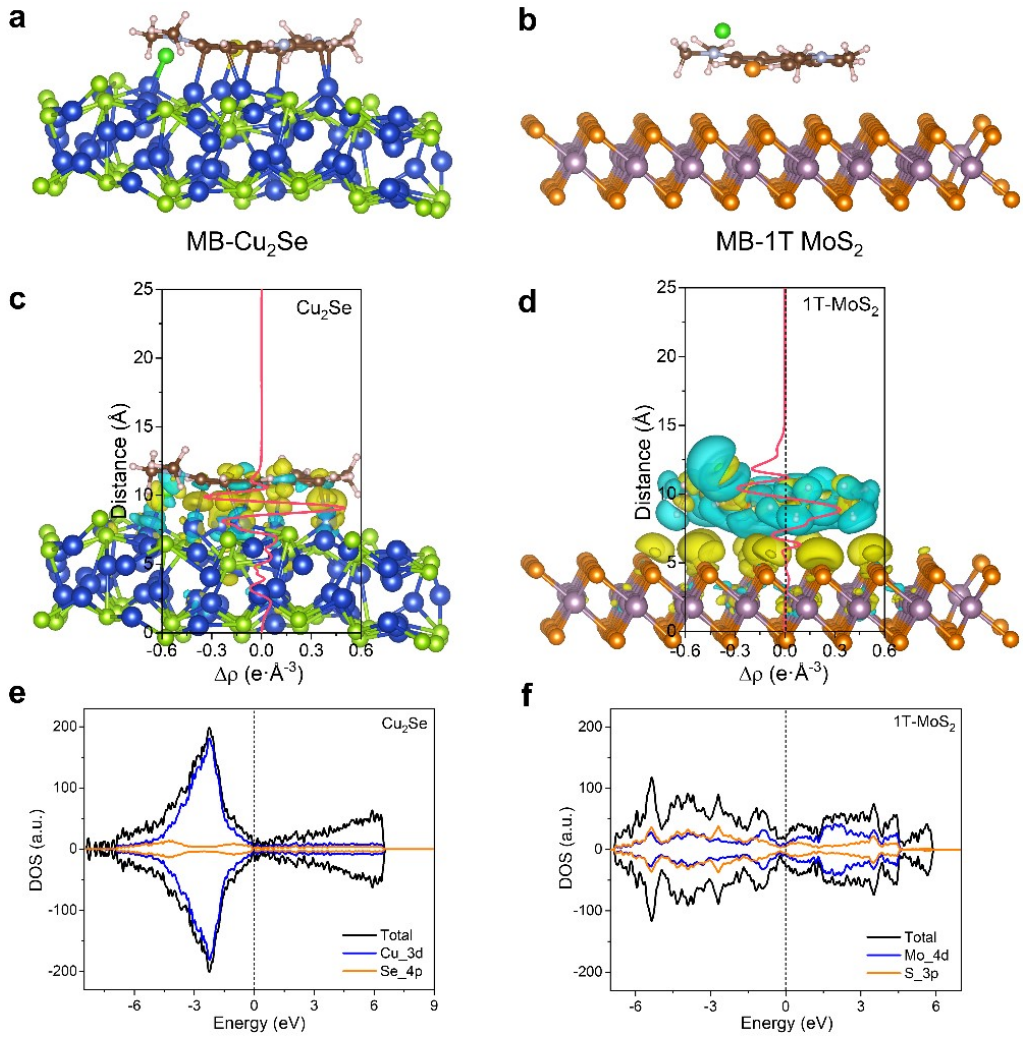

Figure S11. DFT calculations of interfacial electronic coupling in the MB/Cu_2Se and MB/1T-MoS_2 systems. (a, b) Optimized adsorption configurations of MB on Cu_2Se and 1T-MoS_2, respectively. (c, d) Charge density difference plots and the corresponding plane-averaged charge density difference profiles for the MB/Cu_2Se and MB/1T-MoS_2 interfaces, respectively. Yellow and cyan isosurfaces represent electron accumulation and depletion, respectively. (e, f) Projected DOS of the MB/Cu_2Se and MB/1T-MoS_2 systems, respectively.

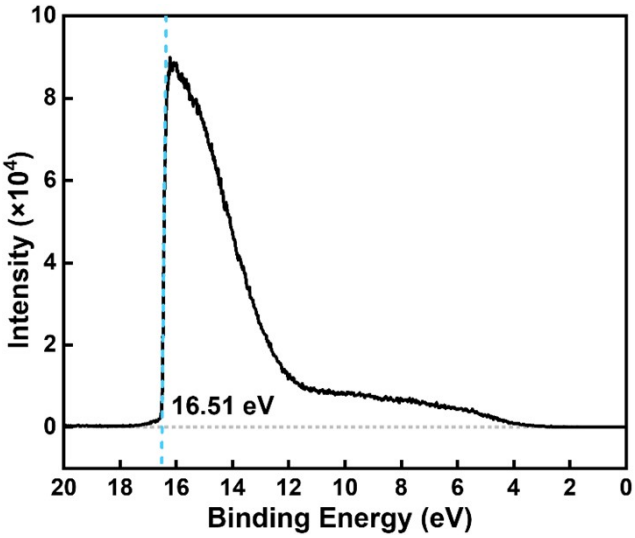

Figure S12. Secondary electron cutoff region in the UPS spectrum of Cu_2Se nanoflakes.

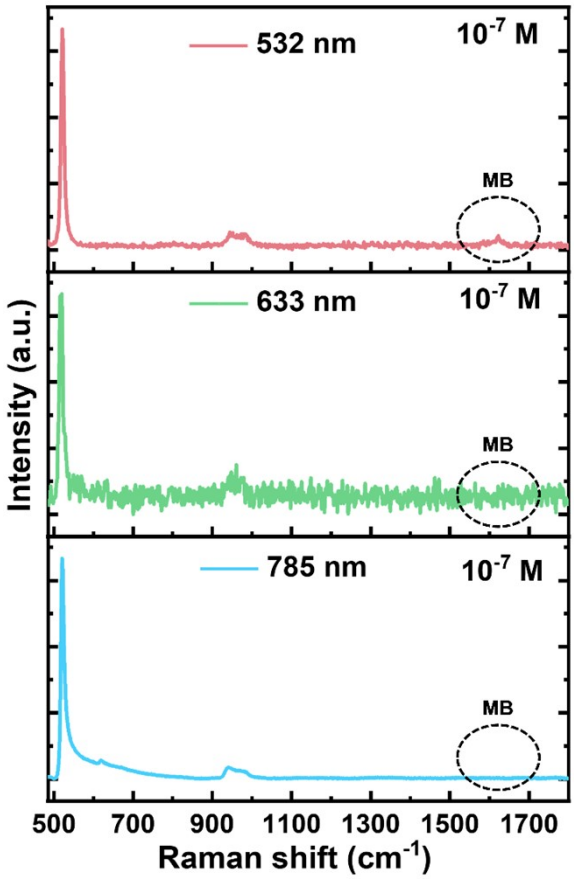

Figure S13. Raman spectra of MB (10^{-7} M) on Cu_2Se nanoflake under excitation at 532, 633, and 785 nm.

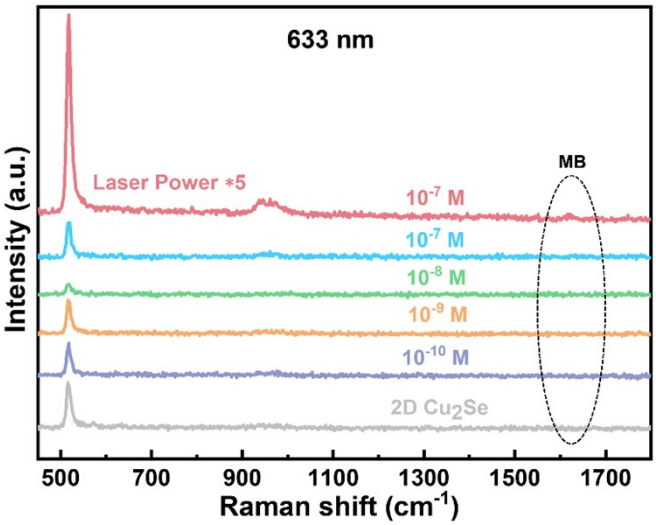

Figure S14. Raman spectra of MB with different concentrations ranging from 10^{-7} to 10^{-10} M on Cu_2Se nanoflake excited under 633 nm laser excitation. For the top curve, the laser power is increased by 5-fold relative to that used for other spectra.

Table S1. Comparison of SERS performances based on various reported 2D metallic materials with this work.

2D Metallic Substrate	Analyte	LOD [M]	EF	Ref.
Ta_4C_3 MXenes	R6G	10^{-7}	1.51×10^5	33
	CV	10^{-6}	N/A	
Nb_4C_3 MXenes	R6G	5×10^{-7}	0.52×10^5	33
Ti_3C_2 MXenes	MB	10^{-7}	2.9×10^6	38
Multilayer 2M-WS_2	CV	10^{-8}	N/A	S1
	BCB	10^{-8}	N/A	
	MB	10^{-8}	N/A	
	MG	10^{-7}	N/A	
	PhB	10^{-6}	N/A	
1T'-$MoTe_2$ films	MB	10^{-8}	1.1×10^8	39
1T-MoS_2	R6G	10^{-9}	2.92×10^4	40
	CV	10^{-8}	2.87×10^4	
1T'-$MoTe_2$	β-sitosterol	10^{-9}	10^4	41
1T'-$MoTe_2$ films	R6G	10^{-9}	1.9×10^6	42
$NbTe_2$	R6G	10^{-9}	5.59×10^6	43
$TaSe_2$ films	R6G	10^{-10}	N/A	S2
	Blirubin	0.316×10^{-6}	N/A	
δ-MoN films	R6G	10^{-10}	1.5×10^7	44
	MB	10^{-9}	N/A	
4L $PtTe_2$	R6G	10^{-10}	N/A	S3
	CV	10^{-10}	N/A	
	RhB	10^{-10}	N/A	
VO_2	R6G	10^{-10}	6.7×10^7	45
Cu_2Se nanoflake	MB	10^{-10}	4.6×10^8	This work
	CV	10^{-10}	N/A	

Reference

S1. Y. Guan, M. Chen, Y. Ding, Y. Fang, F. Huang, C.-Y. Xu, L. Zhen, Y. Li, L. Yang and P. Xu, *ACS Nano*, 2024, **18**, 17339-17348.

S2. Y. Ge, F. Wang, Y. Yang, Y. Xu, Y. Ye, Y. Cai, Q. Zhang, S. Cai, D. F. Jiang, X. Liu, B. Liedberg, J. Mao and Y. Wang, *Small*, 2022, **18**, 2107027.

S3. Z. Lei, D. Wu, X. Cao, X. Zhang, L. Tao, Z. Zheng, X. Feng, L. Tao and Y. Zhao, *J. Alloys Compd.*, 2023, **937**, 168294.